Progress In Electromagnetics Research C, Vol. 94, 59–74, 2019

Enhancement Bandwidth of Half Width-Microstrip Leaky Wave Antenna Using Circular Slots

Mowafak K. Mohsen[1, 2, *], Mohd S. M. Isa[1], Azmi A. M. Isa[1], Muhannad K. Abdulhameed[2], Mothana L. Attiah[1], and Ahmed M. Dinar[1]

Abstract—This paper presents a new technique to enhance impedance bandwidth of single layer half width microstrip leaky wave antenna (HW-MLWA) with continuous main beam scanning. The enhancement is realized by etching four circular slots on the radiation element. Two of the circular slots are placed close to the feed port, and the others are close to the matching load. The wide main beam scanning is between $+12^\circ$ and $+70^\circ$ when operation frequency sweeps between 4.3 GHz and 6.5 GHz. A comparison between the Uniform HW-MLWA (reference) and the proposed HW-MLWA with circular slots is provided to study the effectiveness of the added circular slots. The proposed HW-MLWA is fabricated and tested. The measured impedance bandwidth is 49.9% (4.28 GHz to 7.13 GHz) with peak gain 10.31 dBi at 5 GHz, hence the proposed antenna can be considered as a suitable candidate for C-band applications.

1. INTRODUCTION

The vast growth of the communication system applications and new technologies necessitate the design of wideband antennas to keep pace with such diverse applications [1, 2]. Leaky wave antenna (LWA) is a promising candidate for these developing applications because of its advantages, such as wide bandwidth, low profile, easy fabrication, capability of beam scanning, and narrow beamwidth. LWAs are preferable for use in satellite communication, multipoint communication, and automotive radars [3–7]. In a radar system, most of the applications require a wide bandwidth to reach a continuous wide beam scanning. LWA was discovered in 1940 in a slotted rectangular waveguide, then in 1979, the structure of microstrip leaky wave antenna (MLWA) was proposed by Menzel [8, 9]. Interest in LWAs has endured since it was first discovered. Various types of LWAs have been developed, such as substrate integrated waveguide (SIW)-LWA using line sources for endfire radiation [10], SIW-LWA, such as the butterfly [11], new reconfigurable 1-D LWA Fabry-Perot [12], multilayer SIW composite right left-handed (CRLH) dependent on LWA [13], SIW double periodic CRLH LWA [14], circularly polarized half-mode SIW (HM-SIW) [15], LWA based on SIW with transverse slotted rectangular waveguide [16], novel 3D half width microstrip based on LWA [17], HW-MLWA with stub loaded for beam steering [18], LWA with loaded shorted via [19], and full width microstrip LWA wideband for two symmetrical beam scanning [20]. However, most studies on LWA have focused on continuous beam scanning without focusing on how the bandwidth can be increased to obtain a wide scanning range. Several designs have focused on overcoming bandwidth limitations [21], and multi-feed was used to increase aperture size, leading to an increase in the bandwidth with fixed gain. However, this design is complex and difficult to fabricate because of the multi-feed. In [22], the authors suggested a novel design to enhance

Received 8 April 2019, Accepted 26 June 2019, Scheduled 12 July 2019

* Corresponding author: Mowafak Khadom Mohsen (mowafak.k.m@gmail.com).

[1] Centre for Telecommunication Research and Innovation (CeTRI), Faculty of Electronic and Computer Engineering (FKEKK), Universiti Teknikal Malaysia Melaka (UTeM), Melaka, Jalan Hang Tuah Jaya 75300, Malaysia. [2] Ministry of Higher Education and Scientific Research, University of Kerbala, Iraq.

the impedance bandwidth with high directivity of the resonant cavity antenna by using two dielectric layers as superstrates. However, in [23] the authors suggested 2-D Fabry-Perot LWAs consisting of two periodic metallo-dielectric arrays over a ground plane to enhance impedance bandwidth. In [24] an HW-MLWA with a periodically loaded u-slot was proposed to attain two bands for forward and backward scanning. Recently, in [25] a transmission line based on CRLH-LWA was investigated. In order to enhance input impedance bandwidth, bandpass filter synthesis technique was utilized to design matching sections. The researchers in [26] suggested to extend the use of the split-ring resonators meta-surface to a wide-angle scanning LWA. The major limitation of this design is complex. However, more recently, the authors in [27] proposed the use of a lens that compensated the dispersion of leaky wave, making a whole broadband antenna. This design reduced the losses and cost at high frequency. However, their dispersive nature integrally produced a beam squint effect in the main lobe.

In this paper, a novel technique to increase the bandwidth of uniform HW-MLWA by using circular slots with continuous beam scanning is proposed and investigated. The HW-MLWA is composed of four etched circular slots on the radiation part of the proposed antenna. This circular slot on the patch of LWA causes a mismatch in the impedance. A new circular slot needs to be etched on the microstrip line near matching port to obtain matching impedance. A uniform HW-MLWA can be used to investigate and compare with new proposed HW-MLWA. The proposed HW-MLWA is fabricated and tested to prove the concept of this technique.

2. ANTENNA CONFIGURATION

The proposed HW-MLWA is shown in Figures 1(a) and (b) which illustrate the top view and feed line, respectively. The proposed antenna uses a Rogers RT5880 substrate with length (L) of 180 mm ($2.52\lambda_o$), width (W) of 40 mm ($0.56\lambda_o$), height (h) of 1.575 mm, permittivity (ε_r) of 2.2, and $\tan\delta = 0.0009$, where λ_o is the free space wavelength at 4.2 GHz. The ground plane dimension is the same as that of the substrate dimension, and the length (l_p) and width (w_p) of the microstrip radiating element are 160 mm ($2.24\lambda_o$) and 11 mm ($0.154\lambda_o$), respectively. The top edge of the HW-MLWA radiating element is connected to the ground plane through a perfect electric wall called (septum) which consists of an array of vias, as shown in Figure 1(a). A septum is used to support the propagation of the first high-order mode to avoid the propagation of fundamental TEM wave [28, 29]. The electric wall of the antenna is constructed using 80 vias, wherein the distance between ttwo centres of vias is $D_v = 2$ mm, and all vias have a diameter of $d = 0.9$ mm. The proposed HW-MLWA is fed from one end, and the other end of the antenna is terminated by a 50 Ω matching load to suppress reflected waves [30]. The dimensions of the SMA connectors are based on commercial standard. The gap (S) between the edge

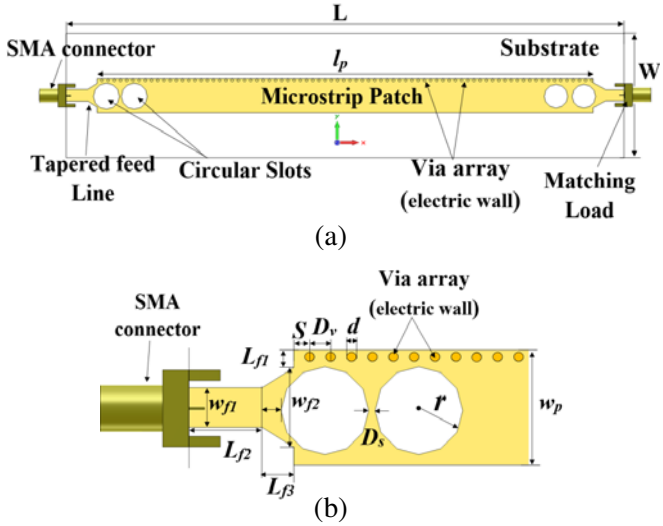

Figure 1. Proposed uniform HW-MLWA. (a) Top view. (b) Tapered feed line and circular slots.

of the microstrip line end and the centre of the first via is important, because it forces the wave toward the microstrip edges (see Figure 1(b)). A tapered feed port is used to improve the matching impedance of the proposed antenna [31]. The dimensions of the tapered feed line (w_{f1}) and (w_{f2}) are determined by using the equations in [32]. The other dimension length of the tapered lines (L_{f2}) and (L_{f3}) is determined by using the equations in [33]. A parametric study is conducted using the software package CST Microwave Studio for optimization. The parameter values of the simulation results are listed in Table 1. The radiation part contains etchings of four circular slots (two near the feed port in the left side and two near the matching load in the right side). The dimension of radius of circular slot (r) is mentioned in Table 1.

Table 1. Some parameters of proposed HW-MLWA.

Parameter	S	W_{f1}	W_{f2}	L_{f1}	L_{f2}
Size (mm)	1.5	3.8	7.6	1.7	7
Parameter	L_{f3}	D_f	r		
Size (mm)	3	1.8	4.2		

3. THEORY

The HW-MLWA has a small size with the same beam scanning capability beam scanning as the conventional MLWA [34]. The direction of the main beam for uniform HW-MLWA is given by [35]:

$$\theta(f) = \sin^{-1}\left[\frac{\beta(f)}{k_o(f)}\right] \tag{1}$$

where β is the phase constant, and k_o is the wave number of free spaces. The main beam scanning from broadside direction to endfire increases in frequency when $0 < \alpha \leq \beta < k_o$, where α is the attenuation constant [36]. The gain decreases when the beam is near the end fire because of the poor radiation in the end fire. The radiation power is dependent on the length l_p of HW-MLWA and leakage rate α. As observed in Figure 2, the leaky wave propagation has an exponential function when the beam scanning is from the broadside towards the end fire. The radiation efficiency of the proposed HW-MLWA can be determined by [37].

$$\eta_{RAD} = 1 - e^{-2\alpha l_p} = 1 - e^{-4\pi\alpha l_p/k_o\lambda_o} \tag{2}$$

The complex propagation constant on HW-MLWA is obtained as follows [38]

$$k = \sqrt{\omega^2\mu\varepsilon_r - k^2} \tag{3}$$

$$e^{j2kw_p} = -\frac{k - \omega\mu Y}{k + \omega\mu Y} \tag{4}$$

$$Y = \frac{h}{120\lambda_o} + j\frac{k_o\varepsilon_r\Delta w_p}{120\pi} \tag{5}$$

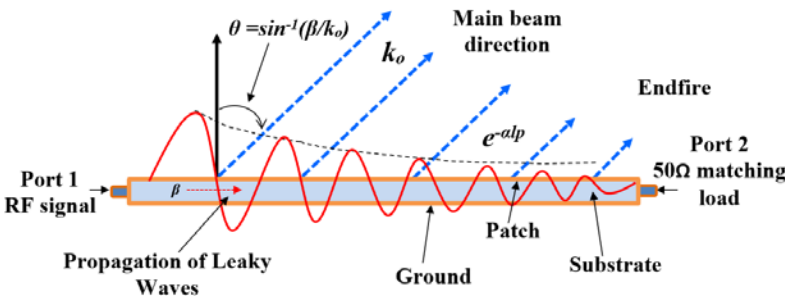

Figure 2. Propagation of leaky wave in uniform HW-MLWA.

where Δw_p is the variable width of the HW-MLWA defined as

$$\Delta w_p = 0.412h\frac{\varepsilon_{eff} + \dfrac{0.3l_p}{h} + 0.262}{\varepsilon_{eff} + \dfrac{0.3l_p}{h} + 0.262} + \frac{D_v}{2\pi}\left[\ln\left(\frac{1}{\pi d/2}\right) - \frac{4\pi^2\left(\dfrac{d}{2}\right)^2}{D_v} + 0.601\frac{D_v^2\varepsilon_r}{\lambda_o^2}\right] \tag{6}$$

$$\varepsilon_{eff} = \frac{\varepsilon_r + 1}{2} + \frac{\varepsilon_r - 1}{2}\left(1 + \frac{5h}{w_p}\right)^{-1/2} \tag{7}$$

An etched circular slot is placed in the radiation element of uniform HW-MLWA to realize wideband antenna. The slot does not increase the size of the antenna and has a small effect on the radiation pattern. The position and shape of the slot on the LWA must be appropriate. Figure 3 shows the RCL equivalent circuit of the proposed antenna. Hence, the equivalent circuit of the circular slot containing inductance with capacitance is a series $L_{s1}C_{s1}$ connected to another $L_{p1}C_{p1}$ shunt. The proposed HW-MLWA has four slots coupled with the RCL equivalent circuit of the radiation element. The equivalent circuit of array vias is inductance-connected parallel to the radiation element. The feed network represented as L_f inductance of the connector is a connected series with a radiation element circuit.

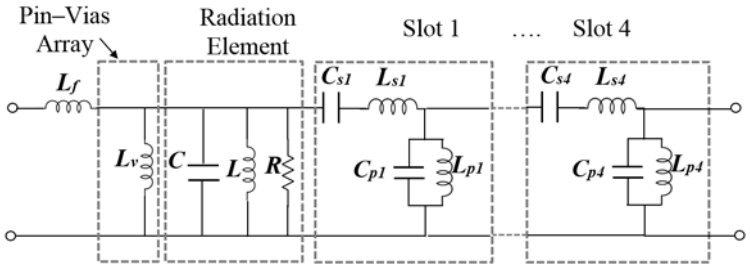

Figure 3. The equivalent circuit of proposed HW-MLWA with circular slots.

In order to calculate the bandwidth of proposed HW-MLWA by using the procedure in [24] to find the cutoff frequency of the proposed antenna let $\beta = 0$

$$f_H = \frac{1}{2\pi\sqrt{C_{s4}L_{s4}}} \tag{8}$$

$$f_L = \frac{\sqrt{L_f C L_T\,(3L_T + L_f)}}{2\pi L_f C L_T} \tag{9}$$

where $L_T = \frac{L_v L}{L_v + L}$.

The correlation of the bandwidth (BW) with a quality factor (Q) of the proposed HW-MLWA is given as $BW = 1/Q\sqrt{2}$. The Q is decreased because of the circular slots in the radiation element and the dielectric loss of substrate and conductor losses of the antenna. Based on this correlation, the bandwidth increases when the Q decreases. The etching slot in the radiation element near the feed port leads to a reduction in the large inductive reactance component of the input impedance of HW-MLWA, making it easier to obtain matching impedance. In this design, the capacitive reactance for the circular slots is compensated by the large inductive reactance for shorting array vias. The electric field distributions of the proposed HW-MLWA with and without circular slots are investigated at band range to verify the first higher order mode of the proposed antenna. The introduction of a shorting pin connects the patch and the ground plane, which forces the electric field to zero. Figures 4(a), (b), (c), and (d) illustrate the electric field distributions at 4.5 GHz, 5 GHz, 5.5 GHz, and 6.5 GHz, respectively. The surface electric field at the edge of the circular slot is very strong, whereas it in the HW-MLWA without slot is very weak. An increase in the electric field in the periodic half width antenna with circular slots leads to an increase in bandwidth. Unfortunately, the antenna with a slot causes a decrease in the realized gain but has a limited effect on the radiation pattern.

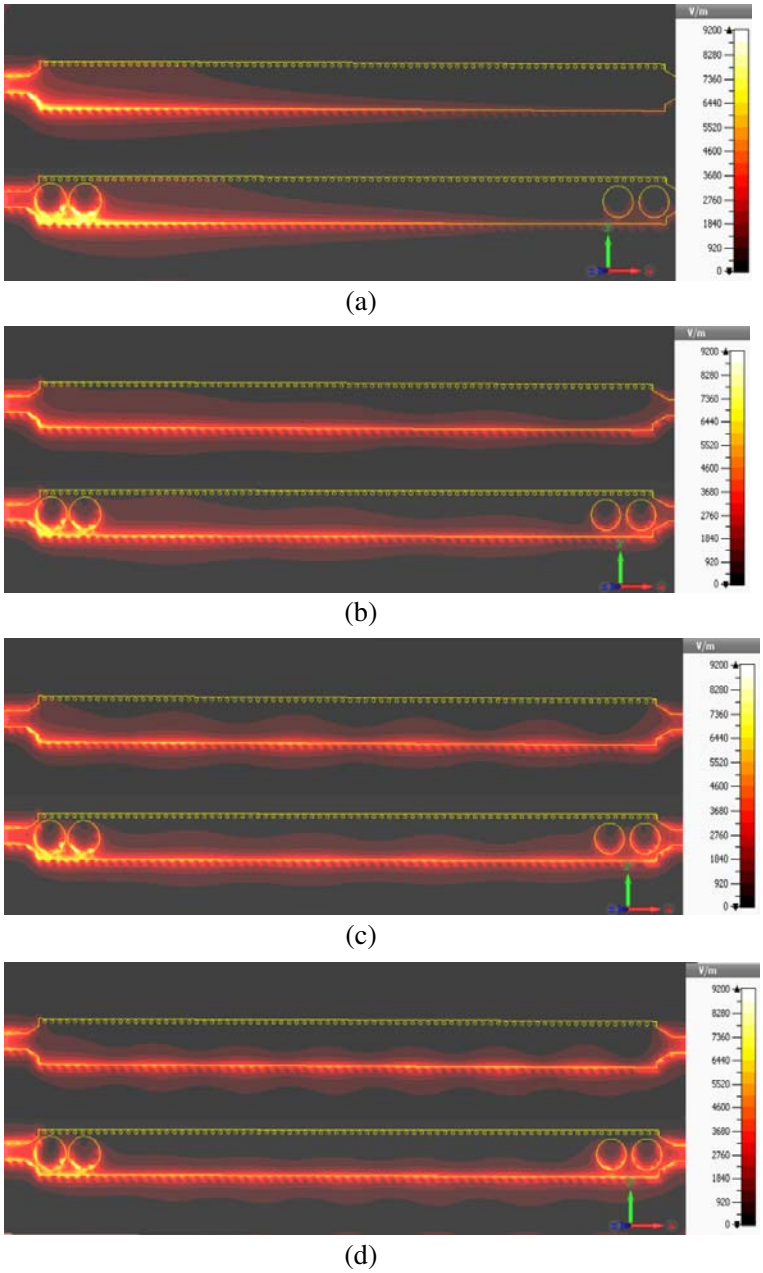

Figure 4. Electric field distributions (amplitude) of two different antennas at: (a) 4.5 GHz, (b) 5 GHz, (c) 5.5 GHz, and (d) 6.5 GHz.

4. RESULT AND DISCUSSION

The proposed HW-MLWA is tested using the CST Microwave Studio. The wideband HW-MLWA is realized by etching circular slots near the feed port and matching port in the radiation element. The etching slots in radiation part do not increase the size of the antenna, and the radiation pattern has a small effect. Figure 5 illustrates the reflection coefficient of HW-MLWA without circular slotting, and Figure 6 shows steps of etching circular slots close to the feed port, leading to an increase in the bandwidth, whereas the etching of circular slots close to the matching load is used to increase the surface current field in the endfire and to match the impedance for proposed antenna. As such, in Figure 5, for the proposed uniform antenna without any slot, the return loss is less than -10 dB from

4.10 GHz to 4.72 GHz and impedance bandwidth 15.3% (4.03 GHz to 4.70 GHz), whereas in Figure 6 the impedance bandwidths of HW-MLWA with one, two, three, and four circular slots are 33.3% (4.40 GHz to 6.16 GHz), 37% (4.40 GHz to 6.40 GHz), 45.8% (4.27 GHz to 6.81 GHz), and 49.9% (4.28 GHz to 7.13 GHz), respectively.

The standing wave is the companion of the original signal propagating in the antenna and reflected wave. The ratio between these waves is known as the voltage standing wave ratio (VSWR). This parameter is used to describe the performance of the proposed antenna with a transmission line. It

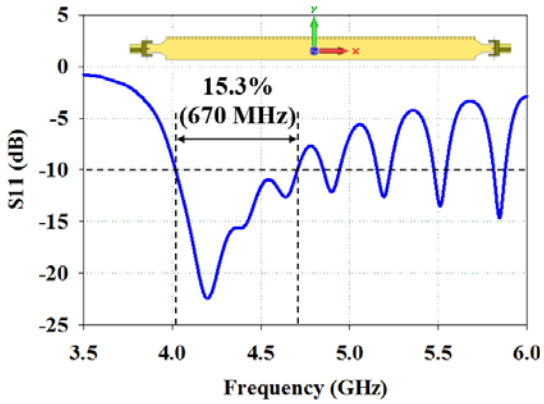

Figure 5. $|S_{11}|$ for proposed HW-MLWA without circular slots.

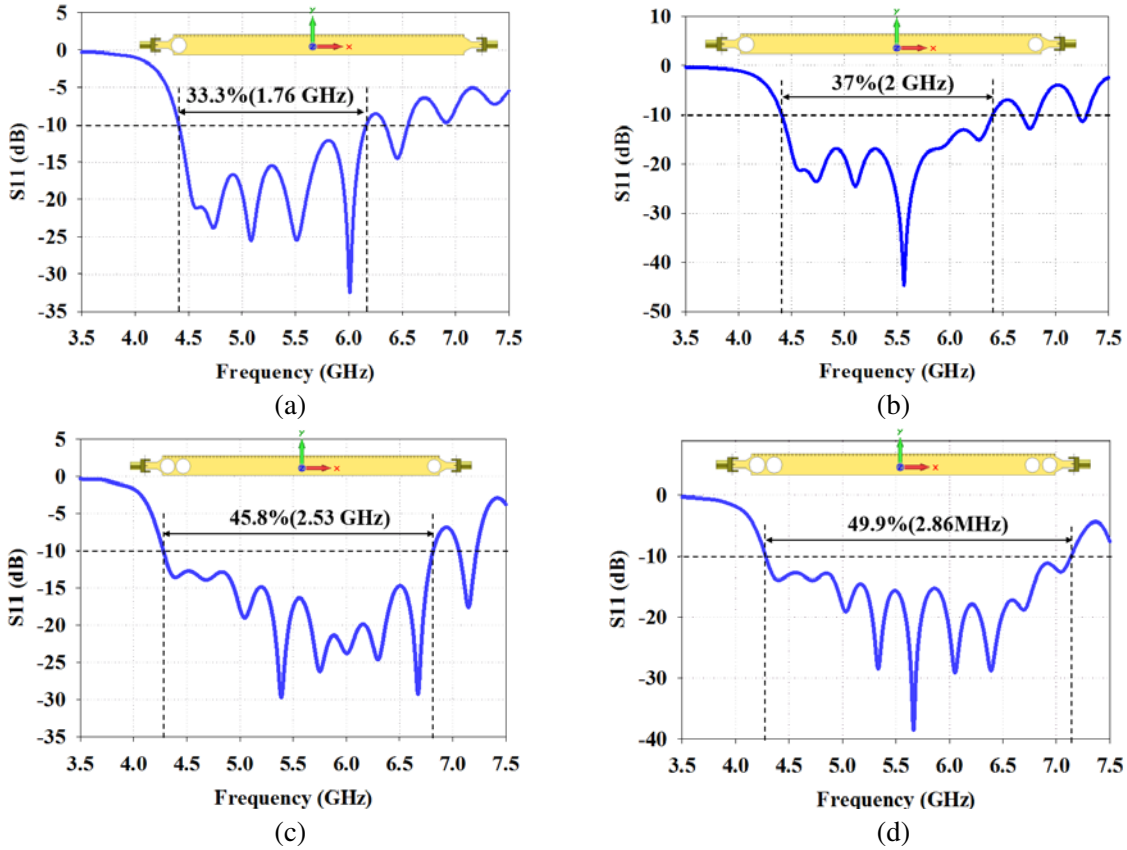

Figure 6. $|S_{11}|$ for proposed HW-MLWA with: (a) One slots. (b) Two slots. (c) Three slots. (d) Four slots.

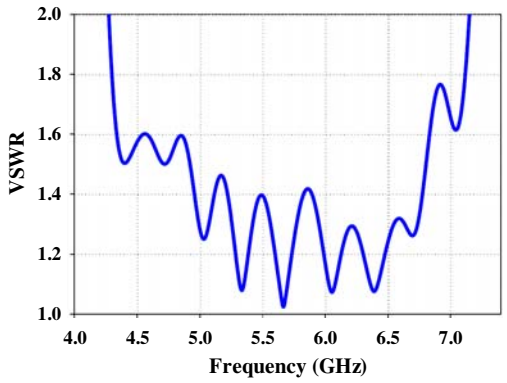

Figure 7. VSWA for the proposed uniform HW-MLWA.

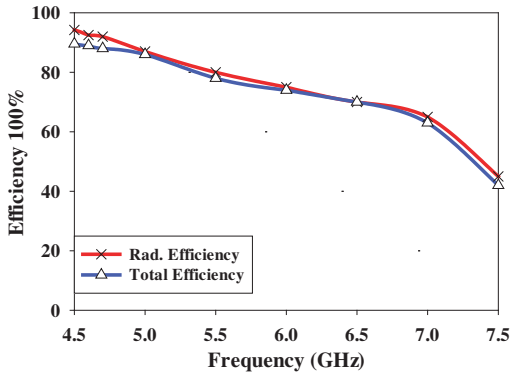

Figure 8. Radiation and total efficiency (%) of the proposed HW-MLWA.

is also used to measure the characteristic impedance of the transmission line and matche the terminal impedance of the proposed antenna. The VSWR is the ratio between the maximum RF voltage and the minimum one along the transmission line. Figure 7 shows that the VSWR is ≤ 2, which means that the proposed antenna has good matching impedance.

The radiation efficiency of the proposed design decreases gradually when the main beam direction becomes closer to the endfire and is high near broadside [24]. The radiation efficiency is decreased by 27.38% when the main beam scanning changes the operating frequency between 4.5 GHz and 7.1 GHz, see Figure 8. The total efficiency of the proposed antenna is close to the radiation efficiency throughout the main beam scanning between 12° and 60° when the frequency changes from 4.5 GHz to 7.1 GHz, indicating good matching throughout scanning range. The total efficiency and radiation efficiency drop at a higher frequency (after 7.1 GHz) because of poor radiation and impedance mismatching at endfire. The decrease in radiation efficiency compensates the high directivity for the proposed HW-MLWA.

4.1. Reduction of the Cross Polarization

The cross-polarization increases significantly when the main beam scanning from broadside to the forward direction and from lower frequencies to the higher frequencies. This is the major limitation of uniform MLWA [31]. Increase in cross polarization levels causes a distortion in the signal quality. As can be seen from Figure 9(a), the distribution of electric field component direction at the edge of

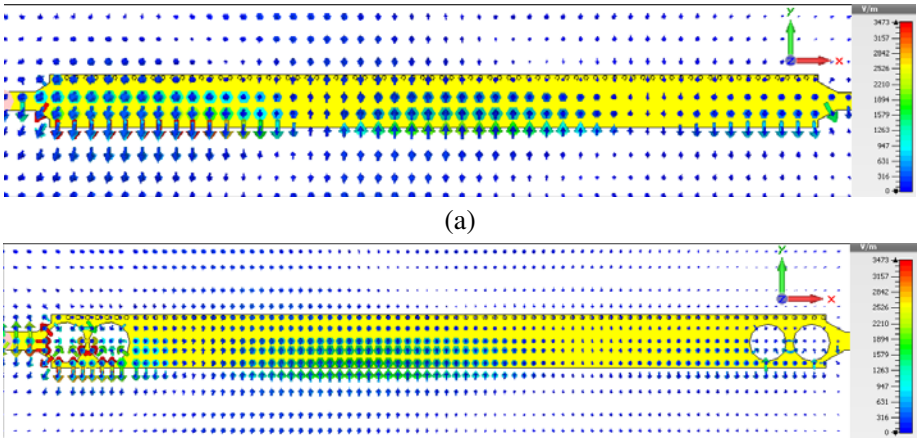

(a)

(b)

Figure 9. Electric field components distribution at 4.5 GHz for: (a) Uniform HW-MLWA. (b) Uniform HW-MLWA with slots.

microstrip line is in y-direction. The field components close to feed port are circularly polarized, and this phenomenon leads to increase of the cross-polarization level in the uniform MLWA. However, the authors in [39] used a balanced symmetric structure around the centre line of the suggested structure, and this technique reduces the cross-polarization level. Our research uses etching circular slots on the radiation elements close feed port which leads to changing the direction of electric field components and hence matching the circular slot with characteristic impedance of the uniform MLWA (see Figure 9(b)). Through this approach, we also achieve good tradeoffs between the cross-polarization and open stopband of MLWA.

The shape of the slot on the radiation element is very critical. The proposed design uses a circular slot to increase the bandwidth with good matching impedance and decrease the cross polarization of the antenna. Figure 10 shows the cross-polarization of proposed HW-MLWA with the circular slot,

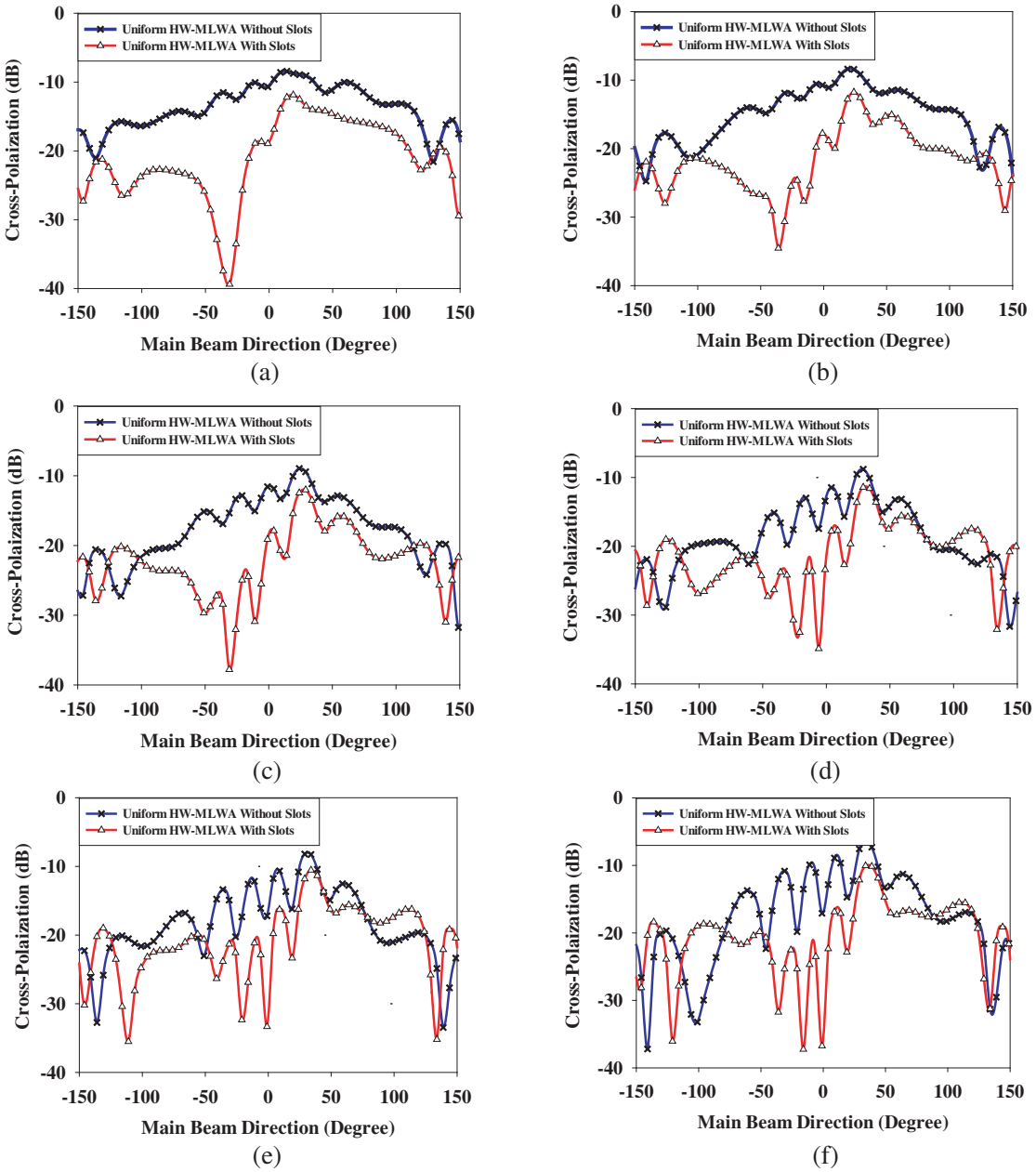

Figure 10. Predicted cross-polarization level of proposed Uniform HW-MLWA with and without slots at: (a) 4.5 GHz, (b) 4.6 GHz, (c) 4.7 GHz, (d) 4.8 GHz, (e) 4.9 GHz, and (f) 5 GHz.

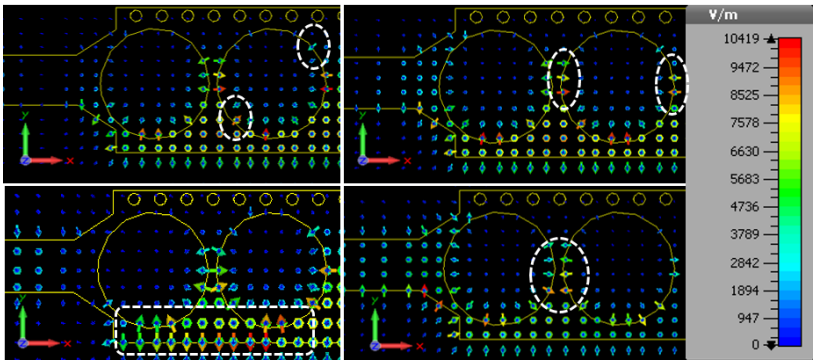

Figure 11. A short section of electric field on the top surface for proposed HW-MLWA with circular slots at 4.5 GHz.

which becomes less than the cross-polarization without slot throughout the main beam scanning by changing the operating frequency (4.5 GHz, 4.6 GHz, 4.7 GHz, 4.8 GHz, 4.9 GHz, and 5 GHz). It can be observed that the cross-polarization increases when the main beam moves to forward direction, from lower frequencies to higher frequencies. Figure 11 illustrates the electric field distribution on the top face of the circular slots on the proposed HW-MLWA (x-y plane) when the main beam direction is $+22^\circ$ at 4.5 GHz. The antenna radiates from the circular slot, which is located in both the polarized directions x and y. The edge of the radiation element also radiates and is polarized in the y-direction. The dashed white circles represent the electric components that cancel each other because these components are in the opposite directions, leading to a decrease in the cross polarization in the proposed antenna.

4.2. Continuous Beam Scanning for the Proposed Antenna

The main beam for the proposed antenna can scan by changing its operating frequency. According to Eq. (1), when a change in the operating frequency results in a change in the value of β/k_o, the main beam direction changes. Various studies have explored LWAs beam scanning by changing the operation frequency [15–15, 40–42]. Although most of these studies have focused on beam scanning, a few studies have focused on increasing the bandwidth which leads to obtaining wide range beam scanning. In Figure 12, the scanning range for the design with circular slots is greater than that without slots. The

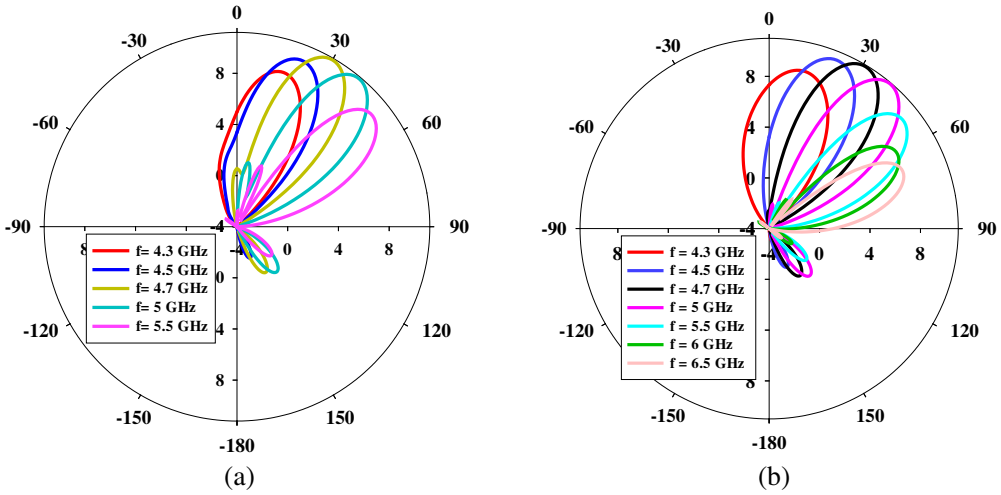

Figure 12. Predicted radiation patterns (x-z-plane) of the proposed HW-MLWA: (a) without circular slots, and (b) with circular slots. (Phi = 0).

boundary bandwidth of the proposed antenna is 4.28 GHz to 7.13 GHz. When the operation frequency between this band and the main beam direction is changed, such as when the elevation angle of the main beam is +12° at 4.3 GHz and the main beam direction +70° at 6.5 GHz, the main lobe is scanned between the broadside and endfire. The realized gain is decreased when the beam scan is close to endfire because of the poor radiation efficiency in endfire. From Figure 12(b) it can be seen that the maximum realized gain of the proposed antenna is equal to 10.31 dBi at 5 GHz with elevation angle +40°.

5. MEASURED RESULTS

The proposed design is fabricated and tested to prove the concept of the proposed wideband HW-MLWA. Figure 13 shows a photo of the fabricated antenna. This section discusses the performance and validation antenna with simulation design in terms of the bandwidth radiation pattern.

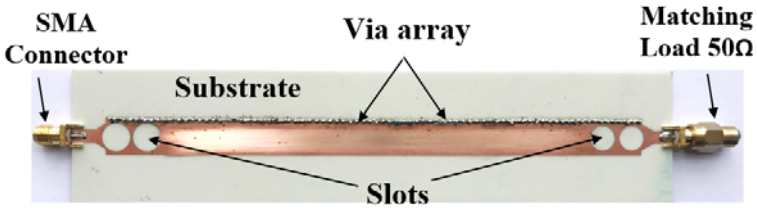

Figure 13. Photograph of the fabricated prototype HW-MLWA.

5.1. *S*-Parameter

The *S*-parameters of the prototype is measured using an Agilent Technologies E5071C Network Analyser. Figure 14 shows that the measured reflection coefficient ≤ -10 dB from 4.32 GHz to 6.86 GHz (45.43%), indicating good agreement between the measured and simulation results. A slight difference can be observed between the simulation and measurement results because the measured curve of the reflection coefficient is shifted marginally in high frequencies. This shifting may occur due to several reasons. First, the losses from the feed connector (SMA) are not included in the CST simulation program. Second, the dielectric and conductor losses in the fabricated proposed antenna are marginally higher than that in the simulation. Finally, the pin-vias in the simulation are replaced by tinned pins in the fabrication, which may lead to an increase in the conductor losses.

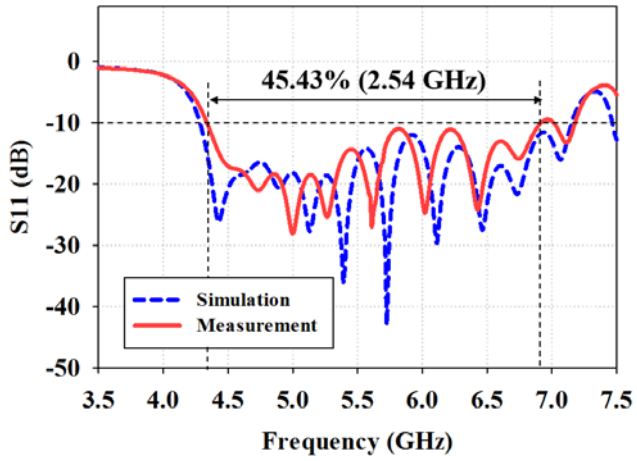

Figure 14. Predicted and measured of reflection coefficient against the frequency of the proposed HW-MLWA.

5.2. Radiation Pattern

The pattern measurement setup is carried out in the Universiti Teknikal Malaysia Melaka (UTeM) /Antenna Measurement Lab (see Figure 15). The measured normalized radiation patterns of the HW-MLWA prototype (x-z plane) are shown in Figures 16(a) and (b) at 4.7 GHz and 5 GHz, respectively. When the operating frequency changes from 4.28 GHz to 7.13 GHz, the simulated main beam scan in the forward direction moves between +12° to +7°. When the frequency increases, the main beam moves from the broadside toward the endfire. The measured radiation pattern is similar to the simulated results. However, a small difference of approximately (3°) is observed in the main beam direction, which could be due to fabrication tolerance, and the measured main beam scan in the forward direction moves between +15° to +73°. Figure 16(a) shows that the simulation result of the main beam direction at 4.7 GHz is +31°, whereas the measured main beam direction at the same frequency is +34°. Figure 16(b) shows the simulation results for the main beam direction at 5 GHz which is at +40° whereas the measurement value is +43°.

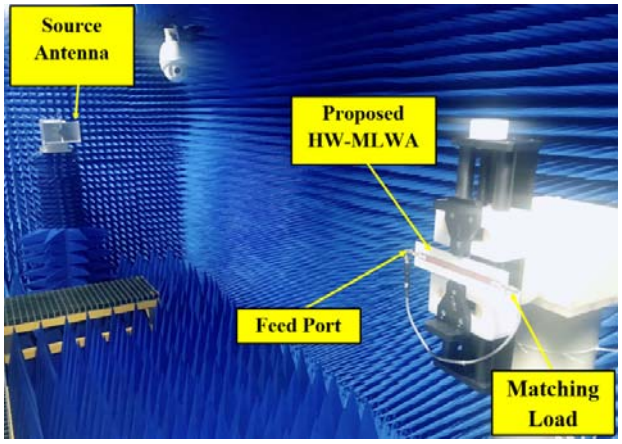

Figure 15. Pattern measurement setup in the Universiti Teknikal Malaysia Melaka (UTeM) (Antenna Measurement Lab).

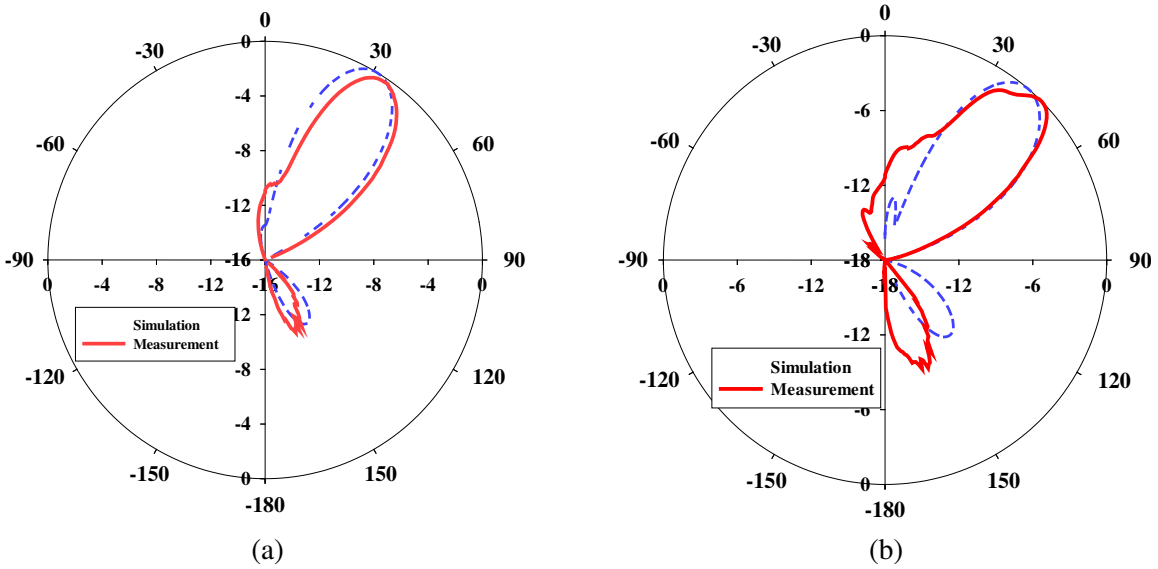

Figure 16. Predict and measured normalized radiation patterns (x-z-plane) of the proposed HW-MLWA with circular slots (Phi = 0) at: (a) 4.7 GHz, and (b) 5 GHz.

5.3. Measured Gain

A compression-method is used to compare the measurement gains of the proposed HW-MLWA (see Figure 17(a)). The measured peak gains at 4.7, 5, 5.5, and 6 GHz are 10.29, 10.31, 9.4, and 7.5 dBi, respectively. At higher frequencies, the gain decreases because of poor matching impedance. The side lobe level is also higher at higher frequencies. However, Figure 17(b) shows that measured gain decreases when the main beam is close to the broadside and endfire.

The main objective of this work is to design a wideband HW-MLWA by using circular slots and achieve continuous beam scanning by changing the operating frequency. However, some interesting characteristics and features were found during the design and measurement process. First, the current distribution of the electric field on the edge of the circular slot mitigates the cross-polarization of the proposed antenna during the change in the main beam direction. Second, the electric field increases with the presence of circular slots, which leads to an increase in bandwidth of the proposed antenna. The proposed design without slot is investigated, and the continuous range scan of the main beam is increased by using circular slots. This work reaches its target by presenting a new type of slot with HW-MLWA. In the design, the number of slots in the proposed antenna is dependent on the matching in the impedance of the antenna. Increasing the number of etching circular slots on the radiation elements (not near the feed and matching port) affects the reactance profile of the antenna, hence the circular slot not matching characteristic impedance of the uniform MLWA, achieving good tradeoffs between the cross-polarization and open stopband of MLWA. Figures 18(a) and (b) show the reflection coefficient

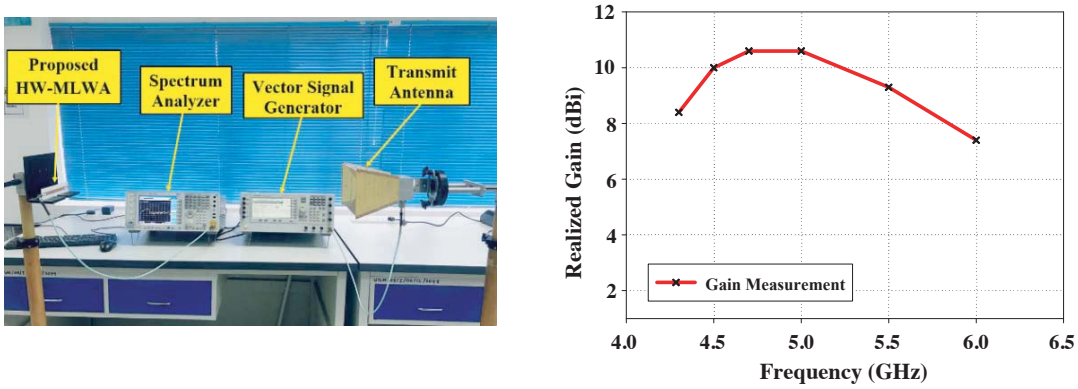

Figure 17. (a) Gain measurement setup of HW-MLWA prototype. (b) Measured gain of the HW-MLWA prototype.

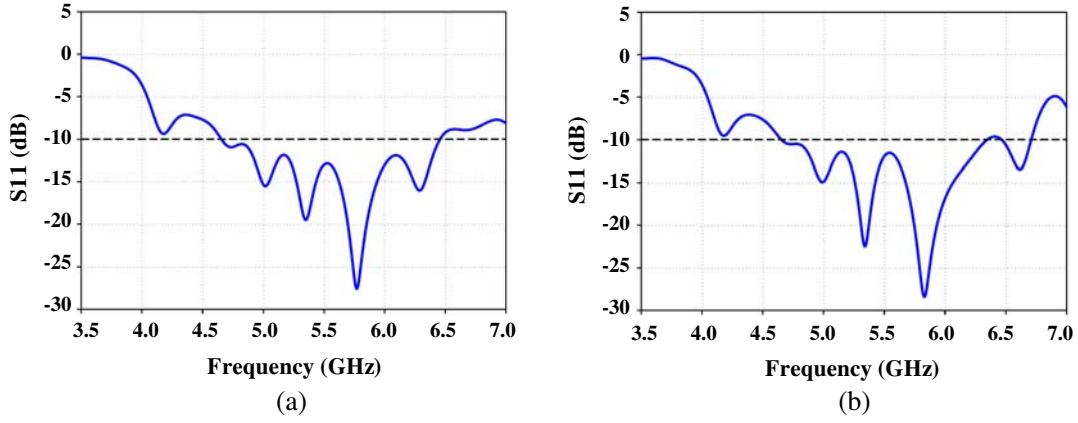

Figure 18. The reflection coefficient against the frequency of the proposed HW-MLWA for: (a) 5 slots. (b) 6 slots.

Table 2. Comparison between the proposed HW-MLWA and reference antennas.

Antenna Reference	Type of Antenna	Broadside Gain	Bandwidth (GHz)	Scanning Range
[24]	HW	-	(5.25 to 6.25) and (7.75 to 9)	Backward to Forward
[34]	HW	~ 1 dBi	$\sim$ (6.1 to 6.6)	$+144^\circ$ to $+41^\circ$
[43]	Fabry-Perot LWA	17.44 dBi	~ 1 GHz	-
[44]	HW	No beam	$\sim$ (6.2 to 6.7)	$+149^\circ$ to $+28^\circ$
[45]	SIW	No beam	$\sim$ (10.2 to 11.5)	Forward only
[46]	HW	No beam	$\sim$ (8.6 to 10.7)	Forward only
[47]	MLWA	No beam	$\sim$ (4.6 to 5.0)	Forward only
[48]	Periodic LWA	9.5 dBi	$\sim$ (23.8 to 24.2)	Broadside Scanning
[49]	MLWA	14.5 dBi	$\sim$ (12.2 to 14.7)	-30° to $+30^\circ$
This work	HW-MLWA	No beam	(4.28 to 7.14)	$+12^\circ$ to $+70^\circ$

against the frequency of the proposed antenna for five and six slots, respectively. Comparisons between the fabrication of this work and some reference antennas are listed in Table 2. These comparisons are in terms of bandwidth, antenna type, the gain in broadside, and scanning range. It is worth to mention here that all the approaches of the references in Table 2 scan the main beam by changing the operating frequency.

6. CONCLUSION

In this work, a new technique to increase the bandwidth of HW-MLWA using a circular slot, from 4.28 to 7.14 GHz, has been proposed. The proposed antenna has generally high radiation efficiency, and the main beam can scan continuously in a forward direction by changing only the operating frequency. This design uses two circular slots close to the feed port and two others close to the matching load. The cross-polarization level decreases because of the circular slots on the radiation element. Finally, the proposed HW-MLWA is fabricated and validated, and the simulation results agree very well with measurements. The measurements of the main beam scanning range from $+15^\circ$ to 73° when the frequency changes from 4.28 to 7.14 GHz. The measured peak gain is 10.31 dBi at 5 GHz. This proposed design is suitable for C-band applications, such as automotive radars.

REFERENCES

1. Attiah, M. L. and I. Ali, "A survey of mmWave user association mechanisms and spectrum sharing approaches: An overview, open issues and challenges, future research trends," *Wirel. Networks*, Vol. 0123456789, 2019.
2. Attiah, M. L., A. A. M. Isa, Z. Zakaria, M. K. Abdulhameed, M. K. Mohsen, and A. M. Dinar, "Independence and fairness analysis of 5G mmWave operators utilizing spectrum sharing approach," *Wirel. Networks*, Vol. 2019, 2019.
3. Sharma, N., and S. Singh Bhatia, "Split ring resonator based multiband hybrid fractal antennas for wireless applications," *AEU — Int. J. Electron. Commun.*, Vol. 93, 39–52, 2018.
4. Alhegazi, A., Z. Zakaria, N. A. Shairi, A. Salleh, and S. Ahmed, "Compact UWB filtering-antenna with controllable WLAN band rejection using defected microstrip structure," *Radio Engineering*, Vol. 27, No. 1, 110–117, 2018.

5. Karmokar, D. K., K. P. Esselle, and S. G. Hay, "Fixed-frequency beam steering of microstrip leaky-wave antennas using binary switches," *IEEE Trans. Antennas Propag.*, Vol. 64, No. 6, 2146–2154, 2016.
6. Mohsen, M. K. Mohsen, M. S. M. Isa, A. A. M. Isa, Z. Zakaria, and M. K. Abdulhameed, "Control radiation pattern for half width microstrip leaky wave antenna by using PIN diodes," *Int. J. Electr. Comput. Eng.*, Vol. 8, No. 5, 2959–2966, 2018.
7. Mohsen, M. K., M. S. M. Isa, Z. Zakaria, A. A. M. Isa, and M. K. Abdulhameed, "Electronically controlled radiation pattern leaky wave antenna array for (C band) application," *Telecommunication, Computing, Electronics and Control, TELKOMNIKA*, Vol. 17, No. 2, 573–579, 2019.
8. Menzel, W., "A new travelling wave antenna in microstrip," *Proc. 8th Eur. Microw. Conf.*, 302–306, Sep. 1978.
9. Mohsen, M. K., et al., "The fundamental of leaky wave antenna," *J. Telecommun. Electron. Comput. Eng.*, Vol. 10, No. 1, 119–127, 2018.
10. Liu, J., D. R. Jackson, Y. Li, C. Zhang, and Y. Long, "Investigations of SIW leaky-wave antenna for endfire-radiation with narrow beam and sidelobe suppression," *IEEE Trans. Antennas Propag.*, Vol. 62, No. 9, 4489–4497, 2014.
11. Mohtashami, Y. and J. Rashed-Mohassel, "A butterfly substrate integrated waveguide leaky-wave antenna," *IEEE Trans. Antennas Propag.*, Vol. 62, No. 6, 3384–3388, 2014.
12. Guzmán-Quirós, R., J. L. Gómez-Tornero, A. R. Weily, and Y. J. Guo, "Electronically steerable 1-d fabry-perot leaky-wave antenna employing a tunable high impedance surface," *IEEE Trans. Antennas Propag.*, Vol. 60, No. 11, 5046–5055, 2012.
13. Nasimuddin, Z. N. Chen, and X. Qing, "Multilayered composite right/left-handed leaky-wave antenna with consistent gain," *IEEE Trans. Antennas Propag.*, Vol. 60, No. 11, 5056–5062, 2012.
14. Jin, C. and A. Alphones, "Leaky-wave radiation behavior from a double periodic composite right/left-handed substrate integrated waveguide," *IEEE Trans. Antennas Propag.*, Vol. 60, No. 4, 1727–1735, 2012.
15. Pourghorban, A. Saghati, M. M. Mirsalehi, and M. H. Neshati, "A HMSIW circularly polarized leaky-wave antenna with backward, broadside, and forward radiation," *IEEE Antennas Wirel. Propag. Lett.*, Vol. 13, 451–454, 2014.
16. Liu, J., D. R. Jackson, and Y. Long, "Substrate integrated waveguide (SIW) leaky-wave antenna with transverse slots," *IEEE Trans. Antennas Propag.*, Vol. 60, No. 1, 20–29, 2012.
17. Gjokaj, V., P. Chahal, L. Kempel, and E. Rothwell, "A novel 3D printed half-width microstrip leaky-wave antenna," *2017 IEEE International Symposium on Antennas and Propagation and USNC-URSI Radio Science Meeting, APSURSI 2017*, Vol. 2017, 1249–1250, Jan. 2017.
18. Karmokar, D. K., D. N. P. Thalakotuna, K. P. Esselle, M. Heimlich, and L. Matekovits, "Fixed-frequency beam steering from a stub-loaded microstrip leaky-wave antenna," *2013 International Symposium on Electromagnetic Theory*, 436–439, 2013.
19. Liu, J., Y. Li, and Y. Long, "Fundamental even leaky mode in microstrip line loaded with shorting vias," *IET Microwaves, Antennas Propag.*, Vol. 11, No. 1, 129–135, 2017.
20. Karmokar, D. K., K. P. Esselle, and T. S. Bird, "Wideband microstrip leaky-wave antennas with two symmetrical side beams for simultaneous dual-beam scanning," *IEEE Trans. Antennas Propag.*, Vol. 64, No. 4, 1262–1269, 2016.
21. Weily, A. R., K. P. Esselle, T. S. Bird, and B. C. Sanders, "Dual resonator 1-D EBG antenna with slot array feed for improved radiation bandwidth," *IET Microwaves, Antennas Propag.*, Vol. 1, No. 1, 198–203, 2007.
22. Al-tari, M. A., et al., "Bandwidth enhancement of the resonant cavity antenna by using two dielectric superstrates," *IEEE Trans. Antennas Propag.*, Vol. 61, No. 2, 1898–1908, 2013.
23. Mateo-segura, C., A. P. Feresidis, S. Member, and G. Goussetis, "Bandwidth enhancement of 2-D leaky-wave antennas with double-layer periodic surfaces," *IEEE Trans. Antennas Propag.*, Vol. 62, No. 2, 586–593, 2014.

24. Karmokar, D. K. and K. P. Esselle, "Periodic U-slot-loaded dual-band half-width microstrip leaky-wave antennas for forward and backward beam scanning," *IEEE Trans. Antennas Propag.*, Vol. 63, No. 12, 5372–5381, 2015.
25. Kushiyama, Y., T. Arima, and T. Uno, "Enhancement of bandwidth for a TL resonator based CRLH leaky wave antenna," *2017 International Symposium on Antennas and Propagation (ISAP)*, No. 3, 3–4, 2017.
26. Cameron, T. R. and G. V. Eleftheriades, "Experimental validation of a wideband metasurface for wide-angle scanning leaky-wave antennas," *IEEE Trans. Antennas Propag.*, Vol. 65, No. 10, 5245–5256, 2017.
27. Wang, L., J. L. Gomez-Tornero, and O. Quevedo-Teruel, "Substrate integrated waveguide leaky-wave antenna with wide bandwidth via prism coupling," *IEEE Trans. Microw. Theory Tech.*, Vol. 66, No. 6, 3110–3118, 2018.
28. Zelinski, G. M., G. A. Thiele, M. L. Hastriter, and M. Havrilla, "Half width leaky wave antennas," *Eur. Sp. Agency, Special Publ. ESA SP*, Vol. 626, 341–348, 2007.
29. Karmokar, D. K., D. N. P. Thalakotuna, K. P. Esselle, L. Matekovits, and M. Heimlich, "Reconfigurable half-width microstrip leaky-wave antenna for fixed-frequency beam scanning," *2013 7th European Conference on Antennas and Propagation, EuCAP 2013*, 1314–1317, 2013.
30. Karmokar, D. K., K. P. Esselle, D. N. P. Thalakotuna, M. Heimlich, and L. Matekovits, "A leaky-wave antenna for beam steering in forward and backward directions," *2013 1st IEEE TENCON Spring Conference, TENCON, Spring 2013*, 47–50, 2013.
31. Karmokar, D. K., Y. J. Guo, P. Qin, S. Chen, and T. S. Bird, "Substrate integrated waveguide-based periodic backward-to-forward scanning leaky-wave antenna with low cross-polarization," *IEEE Trans. Antennas Propag.*, Vol. 66, No. 8, 3846–3856, 2018.
32. Deslandes, D., "Design equations for tapered microstrip-to-substrate integrated waveguide transitions," *IEEE MTT-S Int. Microw. Symp. Dig.*, 704–707, 2010.
33. Lu, K., "An efficient method for analysis of arbitrary nonuniform transmission lines," *IEEE Trans. Microw. Theory Tech.*, Vol. 45, No. 1, 9–14, 1997.
34. Li, Y., Q. Xue, H. Tan, and Y. Long, "The half-width microstrip leaky wave antenna with the periodic short circuits," *IEEE Trans. Antennas Propag.*, Vol. 59, No. 9, 3421–3423, 2011.
35. Chen, T. L., Y. De Lin, and J. W. Sheen, "Microstrip-fed microstrip second higher order leaky-mode antenna," *IEEE Trans. Antennas Propag.*, Vol. 49, No. 6, 855–857, 2001.
36. Lin, Y. and J. Sheen, "Mode distinction and radiation-efficiency analysis of planar leaky-wave line source," *IEEE Trans. Microw. Theory Tech.*, Vol. 45, No. 10, 1672–1680, 1997.
37. Martinez-Ros, J. A., J. Luis Gomez-Tornero, and G. Goussetis, "Planar leaky-wave antenna with flexible control of the complex propagation constant," *IEEE Trans. Antennas Propag.*, Vol. 60, No. 3, 1625–1630, Mar. 2012.
38. Li, Y., Q. Xue, E. K.-N. Yung, and Y. Long, "Quasi microstrip leaky-wave antenna with a two-dimensional beam-scanning capability," *IEEE Trans. Antennas Propag.*, Vol. 57, No. 2, 347–354, Feb. 2009.
39. Wang, Y.-W., Y.-W. Hsu, and Y.-C. Lin, "An X-type CRLH leaky wave antenna with low cross-polarization," *11th European Conference on Antennas and Propagation, EUCAP 2017*, 2180–2183, 2017.
40. Liu, J., D. R. Jackson, and Y. Long, "Substrate integrated waveguide (SIW) leaky-wave antenna with transverse slots," *IEEE Trans. Antennas Propag.*, Vol. 60, No. 1, 20–29, 2012.
41. Nasimuddin, N., Z. N. Chen, and X. Qing, "Substrate integrated metamaterial-based leaky-wave antenna with improved boresight radiation bandwidth," *IEEE Trans. Antennas Propag.*, Vol. 61, No. 7, 3451–3457, 2013.
42. Nguyen-Trong, N., T. Kaufmann, and C. Fumeaux, "A wideband omnidirectional horizontally polarized traveling-wave antenna based on half-mode substrate integrated waveguide," *IEEE Antennas Wirel. Propag. Lett.*, Vol. 12, 682–685, 2013.

43. Mateo-Segura, C., A. P. Feresidis, S. Member, and G. Goussetis, "Bandwidth enhancement of 2-D leaky-wave antennas with double-layer periodic surfaces," *IEEE Trans. Antennas Propag.*, Vol. 62, No. 2, 586–593, 2014.
44. Li, Y., Q. Xue, E. K. N. Yung, and Y. Long, "The periodic half-width microstrip leaky-wave antenna with a backward to forward scanning capability," *IEEE Trans. Antennas Propag.*, Vol. 58, No. 3, 963–966, 2010.
45. Liu, J., D. R. Jackson, and Y. Long, "Substrate integrated waveguide (SIW) leaky-wave antenna with transverse slots," *IEEE Trans. Antennas Propag.*, Vol. 60, No. 1, 20–29, 2012.
46. Losito, O., "High efficiency and broadband microstrip leaky-wave antenna," *Active and Passive Electronic Components*, Vol. 2008, 6 pages, 2008.
47. Chiou, Y., J. Wu, J. Huang, and C. F. Jou, "Design of short microstrip leaky-wave antenna with suppressed back lobe and increased frequency scanning region," *IEEE Trans. Antennas Propag.*, Vol. 57, No. 10, 3329–3333, 2009.
48. Al-Bassam, A., S. Member, S. Otto, D. Heberling, S. Member, and C. Caloz, "Broadside dual-channel orthogonal-polarization radiation using a double-asymmetric periodic leaky-wave antenna," *IEEE Trans. Antennas Propag.*, Vol. 65, No. 6, 2855–2864, 2017.
49. Lyu, Y., F. Meng, G. Yang, P. Wang, Q. Wu, and K. Wu, "Periodic leaky-wave antenna based on complementary pair of radiation elements," *IEEE Trans. Antennas Propag.*, Vol. 66, No. 9, 4503–4515, 2018.